Available online at www.sciencedirect.com
ScienceDirect
Trans. Nonferrous Met. Soc. China 25(2015) 154−161
Transactions of Nonferrous Metals Society of China
www.tnmsc.cn

Thermal conductivity of carbon nanotube−silver composite

Hemant PAL[1,2], Vimal SHARMA[1]

1. Department of Physics, National Institute of Technology, Hamirpur (H.P.) 177005, India;
2. Department of Physics, Govt. Post Graduate College, Chamba (H.P.) 176310, India

Received 3 February 2014; accepted 3 July 2014

Abstract: The molecular level mixing method was extended to fabricate carbon nanotube reinforced silver composite. The influence of type of carbon nanotubes (single/multiwall) reinforcement and their mode of functionalization (covalent/non-covalent) on thermal conductivity of silver composite was investigated. X-ray diffraction and electron diffraction spectroscopy (EDS) confirm the presence of silver and carbon in the composite powder. High resolution scanning electron microscopy and transmission electron microscopy ascertain embedded, anchored and homogeneously implanted carbon nanotubes in silver matrix. Effect of covalent functionalization on multiwall carbon nanotubes was monitored by Raman and Fourier transform infrared spectroscopy. These investigations confirm the addition of functional groups and structural integrity of carbon nanotubes even after covalent functionalization. Thermal conductivity of composites was measured by a laser flash technique and theoretically analyzed using an effective medium approach. The experimental results reveal that thermal conductivity decreases after incorporation of covalently functionalized multiwall nanotubes and single wall carbon nanotubes. However, non-covalently functionalized multiwall nanotube reinforcement leads to the increase in effective thermal conductivity of the composite and is in agreement with theoretical predictions derived from effective medium theory, in absence of interfacial thermal resistance.
Key words: metal matrix composites; carbon nanotubes; thermal conductivity; functionalization

1 Introduction

Silver is an attractive metal due to its high thermal and electrical conductivity. Ag and Ag-graphite composites are used as interconnect and thermal management material in integrated circuits, plug coaters, electric brushes and circuit breakers [1,2]. Carbon nanotubes (CNTs) are considered as versatile filler for fabrications of electrical contact and thermal management materials instead of graphite by virtue of their unique properties. They are characterized by their excellent properties: Real density similar to that of a polymer, with excellent elasticity, high aspect ratio (50−1000) and mechanical strength better than that of steel [3]. Furthermore, extraordinarily low coefficient of thermal expansion (CTE=0) and ultra-high thermal conductivity (3000−6000 W/(m·K)) in combination with the superior electrical and thermal conductivities of the silver [4], CNTs reinforced Ag matrix (CNT/Ag) composites are very attractive to meet the increasing demands for high performance thermal management materials. CNT based metal matrix composites (MMCs) have been reviewed critically by BAKSHI and LAHIRI [5] to summarize the state-of-the-art of this field. They ascertain that the improvement in thermal properties of CNT based MMCs largely depends on the distribution of CNTs and their bonding with matrix. Hence, mode of functionalization of CNTs and processing route are two vital factors that determine thermal properties of the MMCs. Recently, novel molecular-level mixing method has been proposed for achieving a homogeneous dispersion of CNTs in MMCs [6]. This is due to covalent bonding at CNT/metal interface, as a result of strong adherence between surface-modified CNTs and metal ions at the molecular level.

Multiwall carbon nanotubes (M-CNTs) are cheaper than single wall carbon nanotubes (S-CNTs) and better suited to large scale industrial applications, but thermo-physical properties of S-CNTs are much better than those of M-CNTs due to their high effective specific surface area and aspect ratio. In order to efficiently synthesize CNT-based MMCs, it is necessary to disperse CNTs and to activate their graphene structure. CNTs can be

Corresponding author: Vimal SHARMA; E-mail: vml16sharma@yaboo.com.in
DOI: 10.1016/S1003-6326(15)63590-7

activated and dispersed either by covalent or non-covalent functionalization techniques. Covalent functionalization improves dispersion and interfacial bonding of CNTs with metal matrix, but at the same time degrades physical properties of CNTs. On the other hand, non-covalent functionalization of CNTs is accomplished by π stacking interactions of surfactants. This strategy does not degrade inherent properties of CNTs [7]. Therefore, the present work exhibits comparative evaluation of influence of CNT reinforcement on the thermal conductivity of Ag composite in reference to 1) S-CNT/M-CNT reinforcement and 2) covalently and non-covalently functionalized multiwall CNTs (C-CNTs/N-CNTs) reinforcement.

2 Experimental

2.1 Fabrication of CNT/Ag nanocomposite powder

Multiwall and single wall CNTs with purity of 90%−98% as per specifications given in Table 1 were purchased from Nanoshell, USA.

Table 1 Parameters of carbon nanotubes used in synthesis process

Parameter	M-CNTs	S-CNTs
Average diameter/nm	4−12	1−2
Length/μm	15−30	1−10
Purity/%	≥90	≥98
Specific surface area/($m^2 \cdot g^{-1}$)	90−350	350−450
Bulk density/($g \cdot cm^{-3}$)	0.05−0.017	0.17−0.030
Volume resistivity/(Ω·cm)	0.1−0.15	0.1−0.15

A part of multiwall CNTs were covalently functionalized and rests of them were treated with surfactant, sodium dodecyl sulphate (SDS), known as non-covalent functionalization. In covalent functionalization, M-CNTs were treated with $V(H_2SO_4):V(HNO_3)$=3:1 solution for 2 h and subsequently washed many times with de-ionized water and dried in an oven at 120 °C. In non-covalent strategy, CNTs were sonicated in ethanol in presence of SDS for 2 h. C-CNTs and N-CNTs obtained by respective functionalization process were used in synthesis process. Metal salt was reduced chemically instead of thermal reduction as a modification in molecular level mixing method. The synthesis process is called as modified molecular level mixing method [8]. C-CNTs and N-CNTs were dispersed in 200 mL ethanol by probe sonication. $AgNO_3$ (Sigma Aldrich, purity 99 %) was taken as metal salt for synthesis of MMCs. 3 g silver nitrate was poured in the dispersed CNT solution with magnetic stirring for 12 h. 2 mL hydrazine hydrate (Merck, purity 99%−100%) was added to this solution as a reducing agent. All chemicals employed in synthesis process were of analytical reagent grade and used without further purification. The resultant solution was centrifuged and precipitates were washed many times with de-ionized water to remove surfactant completely. Finally, CNT/Ag nanopowder was obtained by drying the precipitates at 50 °C on a hot plate. S-CNT/Ag nanocomposite samples were also prepared by following the same procedure.

2.2 Consolidation of CNT/Ag nanocomposite powder

The nanopowder was compacted by uniaxial molding press at a pressure of 320 MPa. Pellets of dimensions *d*13 mm×2 mm of CNT/Ag nanocomposites containing 0, 3%, and 6% CNTs (volume fraction) were prepared. All fabricated nanocomposite samples were sintered in horizontal tube furnace with attached programmable temperature controller. Composite samples were placed in alumina tube by keeping them in silica crucible. Sintering temperature of 800 °C was attained at sintering rate of 5 K/min in an inert atmosphere. Sintering temperature was kept constant for 12 h. Theoretical and measured densities of samples evaluated after sintering are tabulated in Table 2.

Table 2 Relative density of CNT/Ag samples after sintering

Composition	Theoretical density/ ($g \cdot cm^{-3}$)	Measured density/ ($g \cdot cm^{-3}$)	Relative density/%
Ag	10.40	10.20	97.23
N-CNT (3%)/Ag	10.22	9.57	93.63
N-CNT (6%)/Ag	9.96	9.14	91.76
C-CNT(3%)/Ag	10.22	9.73	95.20
C-CNT(6%)/Ag	9.96	9.05	90.86
S-CNT (3%)/Ag	10.22	9.53	93.24
S-CNT (6%)/Ag	9.96	9.02	90.56

2.3 Sample characterization

X-ray diffraction patterns of powdered samples were recorded with a Panalytical 3050/60 Xpert-PRO using Cu K_α radiation. Microstructure of the samples was studied using scanning electron microscope (SEM) FEI Quanta FEG 450 and transmission electron microscope (TEM) JEOL JEM 2100F operated at 200 kV. FTIR spectra were recorded in IR region of 1000−4000 cm^{-1} by Perkin Elmer SP-65 and Raman spectra were observed in the range of 1000−1800 cm^{-1} by Reins haw In via Raman microscope. Thermal conductivity was measured by using the following formula:

$$K_e = \alpha \rho c_p \quad (1)$$

where K_e is the effective thermal conductivity, α is the thermal diffusivity, c_p is the specific heat and ρ is the density of consolidated samples obtained at room temperature. The thermal diffusivity was measured using

a NETZSCH LFA 447 Nano Flash^{TM} diffusivity apparatus. It was equipped with a furnace capable of operation from 25 to 300 °C, software controlled automatic sample changer and an In-Sb detector.

3 Microstructural characterization

In molecular level mixing process, nucleation of nanoparticles occurs in stable CNTs suspension. It leads to homogenous dispersion of embedded CNTs in MMCs at the molecular level. Therefore, confirmation of presence of silver nanoparticles and CNTs in MMCs powder was carried out by X-ray diffraction (XRD) and electron diffraction spectroscopy (EDS). Figure 1(a) displays XRD pattern of CNT/Ag nanocomposite. It indicates crystalline nature of nanocomposite. The peaks at 2θ=38.9°, 45.1°, 65.1°, 78.2° and 82.4° correspond to (111), (200), (220), (311) and (222) reflections of silver as per JCPDS (file No. 04-0783) data. A weak peak at 2θ=26.5° indicates the presence of CNTs in nanocomposite.

The quantitative presence of carbon and silver in the nanocomposite powder is indicated by EDS characteristic profile of CNT/Ag nanocomposite (Fig. 1(b)). The peaks observed at 3.0, 3.2 and 3.4 keV correspond to binding energies of Ag while the peak situated at the binding energy of 0.25 keV corresponds to C.

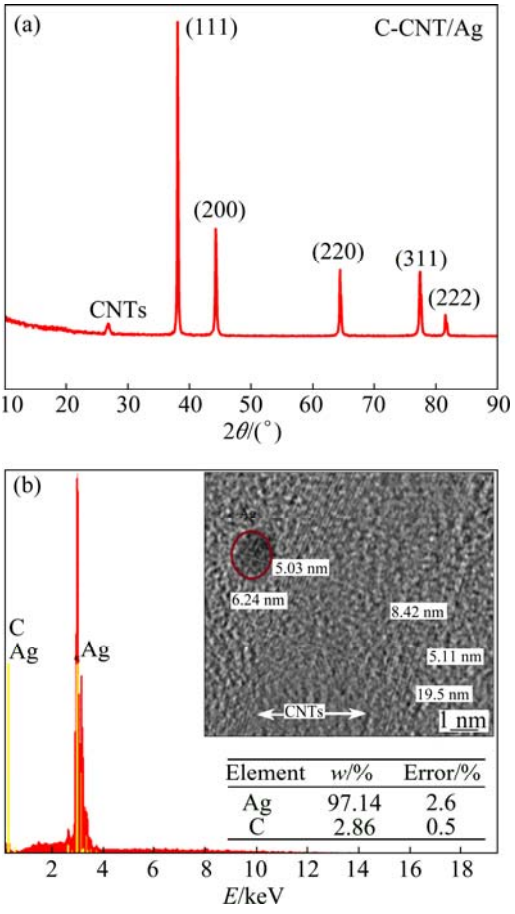

Fig. 1 XRD pattern of C-CNT (6%)/Ag nanocomposites (a) and EDS spectrum of C-CNT (3%)/Ag nanocomposite (b)

In order to examine microstructure of composites, thorough microstructural characterization of fabricated nanocomposites was carried out by means of SEM and TEM. SEM images of nanocomposite powder are displayed in Fig. 2. Homogenously dispersed and bonded multiwall C-CNTs in silver matrix are indicated in Fig. 2(a). The most important feature is that multiwall C-CNTs are decorated with silver nanoparticles interconnected in a network like structure. Obviously, this type of network structure enables CNTs to bond strongly with matrix. S-CNTs are more or less homogenously dispersed in the matrix but few agglomerates are also visible (Fig. 2(b)).

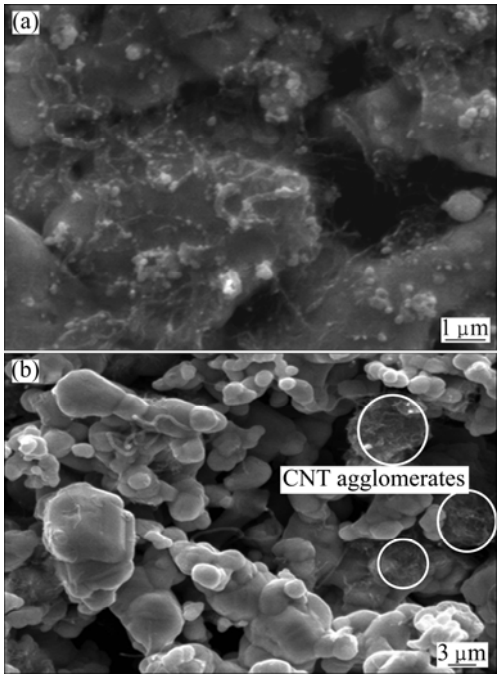

Fig. 2 SEM micrographs of C-CNT (3%)/Ag (a) and S-CNT (3%)/Ag nanocomposite (b)

TEM micrograph of dispersed C-CNT/Ag nanocomposite in ethanol before consolidation is shown in Fig. 3(a). The defected sites of C-CNTs and attached Ag powder are highlighted. Embedded, intact N-CNT and S-CNT in silver matrix are also clearly visible in Figs. 3(b) and (c). The chemical bondings formed due to covalent functionalization between Ag and C-CNTs during molecular level mixing process are displayed in FTIR spectra.

Figure 4(a) shows FTIR spectra of N-CNTs, C-CNTs and C-CNT/Ag nanocomposites. The individual spectrum is vertically shifted with purpose of improving visualization effect. Small peaks around 1060 cm^{-1} and 3400−3500 cm^{-1} corresponding to C—O/C—C and

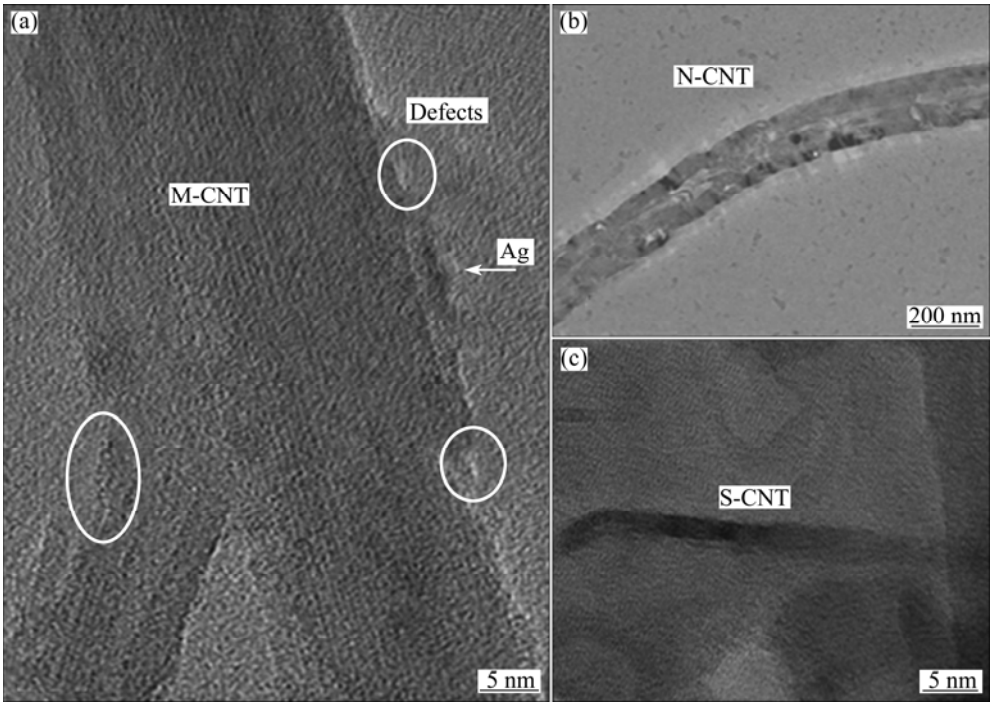

Fig. 3 High resolution TEM micrographs of C-CNT/Ag (a), N-CNT/Ag (b) and S-CNT/Ag nanocomposite with 3% CNTs (c)

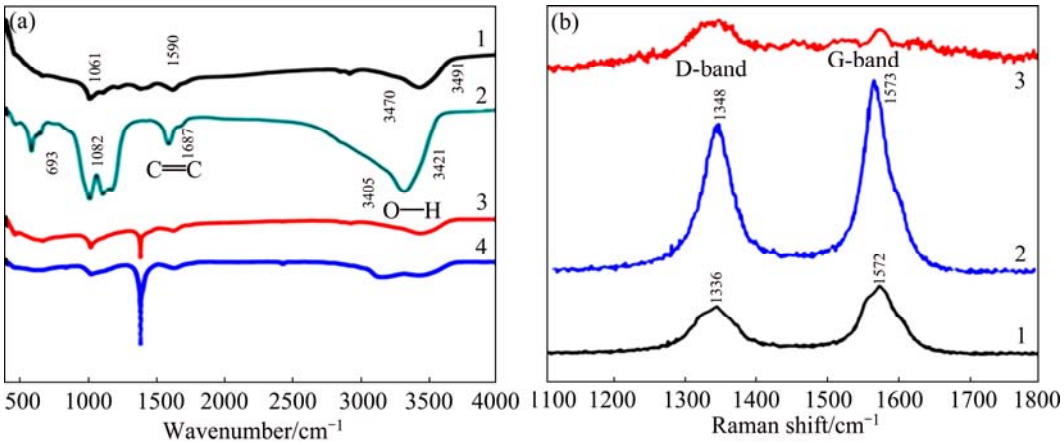

Fig. 4 FTIR spectra (a) and Raman spectra (b) of carbon nanotube-silver composites: 1—N-CNTs; 2—C-CNTs; 3—C-CNT (3%)/Ag; 4—C-CNT (6%)/Ag

O—H bonds stretching are initially presented in pristine CNTs. IR spectrum of C-CNT shows prominent absorption peak around 1687 cm^{-1} corresponding to stretching vibration of C═C from carboxylic groups (—COOH) and carbonyl characteristic peak. Broad peaks at 1061−1082 cm^{-1} could be assigned to C—O and C—C bonds stretching. Peak at around 3445 cm^{-1} can be assigned to O—H stretching vibrations of carboxyl groups (O═C—OH and C—OH) due to oxidation of some carbon atoms on the surfaces of CNTs by nitric and sulphuric acids. Aromatic C═C stretch is observed at around 1590 cm^{-1} in spectra. The presences of oxygen-containing functional groups are in abundant on the surface of C-CNTs [9]. These results indicate that outer surface of CNTs is modified through oxidation by H_2SO_4−HNO_3 with some functional groups [10]. These functional groups are chemically active, which may act as a catalytic function to ensure the metal ions adherence to CNT surface. No change in FTIR spectra of pristine nanotubes has been found in the case of non-covalent functionalization. However, in IR spectrum of C-CNT/Ag nanocomposite, peak positions are shifted and are found to be different from those of both the N-CNTs and C-CNTs, which is a clear indication of interaction of CNTs with silver. The suppression of prominent absorption peaks of C-CNTs at 1031, 1631 and 3421 cm^{-1} in silver composite are correlated with stretching of bonds due to interaction between CNTs and metal particles. The appearance of a peak approximately at 1400 cm^{-1} corresponds to the C—O stretching,

indicating the interaction and perturbation at the CNT surface due to adherence of metal particles [11].

Raman spectroscopic measurements are carried out to assess the structural integrity of CNTs. Figure 4(b) shows the Raman spectra of N-CNTs and C-CNT along with C-CNT/Ag nanocomposite recorded at room temperature and ambient pressure. Two features in the first-order Raman spectra are a G-band at 1570−1580 cm^{-1} revealing two-dimensional graphitic ordering of nested graphene layers of C-CNTs and a D-band at 1340−1350 cm^{-1} which is highly responsive to non-planar atomic distortions, amorphous carbon, C-CNT curvature and other carbon impurities. The slight increase in D to G peak intensity ratio indicates that covalent functionalization has increased defect density by introducing carboxylic, carbonyl and hydroxyl groups. These results indicate certain insertion of defects and/or break in structure of C-CNTs. The presence of broad G band shoulder in spectra of C-CNT/Ag nanocomposite indicates bond-angle distortion at the C-atom in six fold aromatic rings, due to covalent functionalization and interaction between silver with CNT surface [12].

4 Results and discussion

Figure 5 shows the variation of thermal conductivity of CNT/Ag nanocomposite in comparison with unreinforced Ag, in the temperature range from 200 to 300 °C. The average thermal conductivity variation as a function of CNT volume fraction is normalized as K_e/K_m, where K_e is the effective thermal conductivity of the CNT/Ag composites and K_m is the thermal conductivity of unreinforced Ag (Fig. 6).

It is generally accepted that thermal properties of composites are dominated not only by the reinforcement and matrix but also by synthesis method as well as interfacial bonding status between them. Composites prepared by powder metallurgy, particle compositing process and molecular level mixing method using

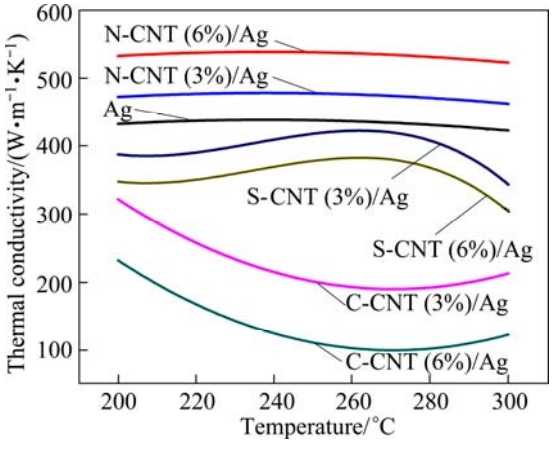

Fig. 5 Thermal conductivity of CNT/Ag nanocomposite

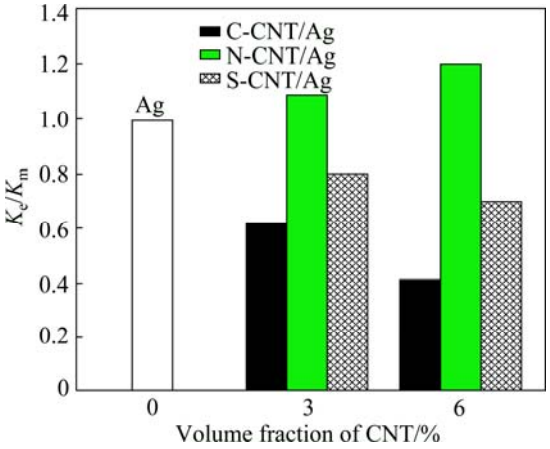

Fig. 6 Comparison of average normalized effective thermal conductivities of CNT/Ag nanocomposites with unreinforced Ag

covalently functionalized CNTs, show decrease in thermal conductivity in reference to pure metal [13−15]. Resultant thermal conductivities of metallic composites prepared by electrochemical deposition are slightly greater than those of pure metals. CHAI and CHEN [16] have developed CNT/Cu composite by electrochemical co-deposition method and reported enhancement in thermal conductivity of about 180% greater than that of Cu. Recently, CHU et al [17,18] have reported the improvement in thermal conductivity of CNT/Cu composite using matrix alloying method. This approach has utilized matrix-alloying element to establish a strong interface between CNT and Cu matrix.

In this work, Figs. 5 and 6 show that C-CNT and S-CNTs reinforcements degrade effective thermal conductivity of CNT/Ag composites. However, in case of N-CNT/Ag nanocomposite, the thermal conductivity increases with increasing CNT volume fraction in silver matrix. This difference in CNT reinforcement behavior is because of the influence of their mode of functionalization, since electrons and phonons both are accountable for effective thermal conductivity of a material. However, their contribution to total thermal conductivity depends upon the nature of material. For covalent materials such as diamond, phonons are a dominant factor in determining total thermal conductivity and contribution of electrons is negligible. Alternately, electrons in metals are a dominant contributor to total thermal conductivity of material and contribution of phonons is very small [16]. Thermal conduction in Ag is due to electrons whereas in CNTs it is due to both electrons and phonons. The fact has been established that chemical treatment of CNTs with strong acids creates defects on its surface due to cleavage of C—C bonding structure. Final products are decorated type nanotubes with various functional groups [19]. This

fact is also confirmed by FTIR and microstructural analysis. Adherence between C-CNTs and metal matrix in MMCs fabricated by molecular level mixing method has been correlated to covalent bonding at CNT/metal interface due to sharing of electrons between surface modified CNTs and metal ions [20]. This covalent bonding between C-CNTs and metal ions might increase mechanical strength but decrease thermal conductivity due to reduction in availability of free electrons for thermal conduction. It is evident from high resolution TEM and Raman spectrum of C-CNTs in MMCs that, the structure of CNTs is distorted to some extent by covalent functionalization. Therefore, when a phonon travels in such C-CNTs, it gets scattered at defect sites leading to the decrease in thermal conductivity.

Although S-CNTs have higher thermal conductivity than multiwall CNTs, their reinforcement has also degraded thermal conductivity of silver composite. S-CNTs are always in the form of strongly bundled ropes due to their high effective surface area. Therefore, it is difficult to disperse S-CNTs homogenously in comparison with multiwall CNTs. Thus, decrease in thermal conductivity of S-CNT/Ag composite might be mainly due to the presence of CNT agglomerates in the composite as evidenced by Fig. 2(b). Low thermal conductivity of C-CNT/Ag and S-CNT/Ag composites may be correlated to combined effect of lattice phonon dissipation due to covalent functionalization, the interfacial thermal resistance between silver and CNT reinforcement, porosity in composite and agglomeration of CNTs [13−15]. However, non-covalent approach involves adsorption of the metal ions on CNT surface, either via weak π–π stacking interaction or through Coulomb attraction without disturbing the free electron system of CNTs. In silver, thermal conduction is dominated by electrons. However, in CNTs, thermal conduction is influenced by phonons as well as delocalized electrons. The N-CNT in conductive metals such as silver may achieve desired thermal conductivity due to lower thermal resistance because of thermal conduction contributions both from phonons as well as uninterrupted delocalized electrons of N-CNTs [21].

In order to understand thermal conductivity behavior of CNT/Ag composites, it is important to compare the experimental results with theoretical predictions. NAN et al [22] has proposed a theoretical model to calculate effective thermal conductivity of CNT based composites in terms of a Maxwell–Garnett effective medium approach. This model assumes random orientation of the dispersed CNTs within the matrix. The effective thermal conductivity (K_e) of CNT based composite assuming a random dispersion of CNTs and a high aspect ratio (p>1000) is given by

$$K_e = K_m(1+\frac{fK_c}{3K_m}) \quad (2)$$

NAN and co-workers [23] further modified theory by incorporating the influence of interfacial thermal resistance as

$$K_e = K_m[1+\frac{fK_c/K_m}{3(P+2R_kK_c/dK_m)}] \quad (3)$$

where d is the diameter of CNTs, R_k=8.3×10^{-8} m^2·K/W is the value of interfacial resistance between the CNTs and metal matrix, experimentally determined by HUXTABLE et al [24].

NAN et al [25] has also developed a more general formulation for the effective thermal conductivity of arbitrary particulate composite with interfacial thermal resistance based on multiple scattering theories:

$$\frac{K_e}{K_m} = \{3(K_x/K_m+1)+f[2(K_x/K_m-1)+(K_x/K_m+1)\cdot (K_z/K_m-1)]\}/[3(K_x/K_m+1)-2f(K_x/K_m-1)] \quad (4)$$

$$K_x = \frac{K_c}{2R_kR_c/d+1},\ K_z = \frac{K_c}{2R_kK_c/L+1} \quad (5)$$

where K_e, K_c and K_m are the thermal conductivities of the composite, the CNT and the matrix, respectively; f is the volume fraction of CNTs; K_x and K_z are effective thermal conductivities of the CNTs along transverse and longitudinal axes, respectively; L is the length of CNT. The thermal conductivity values of silver and CNTs used in the calculation are taken to be 430 and 4500 W/(m·K), respectively. The average diameter and length of CNTs are 8 nm and 20 μm as provided by the supplier, respectively. The comparison between our experiments and theoretical calculations is shown in Fig. 7.

The predictions without considering interfacial thermal resistance (Eq. (2)) show increase in thermal

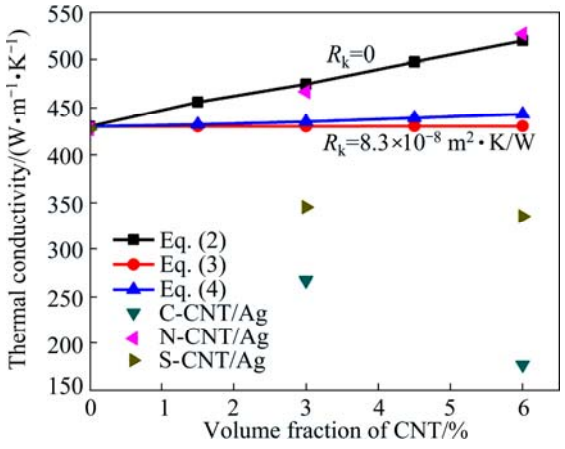

Fig. 7 Comparison between predictions given by Eqs. (2)−(4) and experimental data for thermal conductivity of CNT/Ag composites as a function of CNT volume fraction

conductivity and agree well with the experimental results of N-CNT/Ag nanocomposite. It is shown that N-CNT/Ag nanocomposite exhibits very low interfacial thermal resistance due to non-covalently functionalized CNTs. However, the experimental values of C-CNT/Ag and S-CNT/Ag are even less than the predictions of modified model (Eqs. (3) and (4)), which includes the interfacial thermal resistance. This deviation from theoretical predictions is attributed to the increase in interfacial resistance due to covalent functionalization interactions of the CNTs, which are not considered in theoretical predictions. C-CNTs contain surface defects due to cleavage of C—C bonding that could also scatter the heat flow. More sophisticated theoretical models taking account of all these factors may give a better description.

5 Conclusions

1) CNT/Ag nanocomposites are successfully fabricated by using modified molecular level mixing method. The influence of type of carbon nanotubes (S-CNT/M-CNT) reinforcement and their mode of functionalization (covalent/non-covalent) on thermal conductivity of silver composite is investigated. The silver matrix composites with well embedded and uniformly dispersed CNTs are obtained.

2) The experimental results show that thermal conductivity unusually decreases after the incorporation of C-CNTs and S-CNTs in silver matrix. However, N-CNT reinforcements lead to the increase in effective thermal conductivity of composite, which is also very close to predictions given by effective medium approach, in absence of interfacial thermal resistance.

Acknowledgements

We are grateful for the financial support from Department of Science and Technology [Project-SR/FTP/PS-054/2011(G)], India and Advanced Instrumentation Research Facility (JNU), New Delhi, for HRTEM analysis.

References

[1] DAVID M J, SATTI P S S. Future trends in materials for lightweight microwave packaging [J]. Micro Electronics International, 1998, 15(3): 17−21.

[2] SLEZIONA J, WIECZOREK J, DYZIA M. Mechanical properties of silver matrix composites reinforced with ceramic particles [J]. Journal of Achievements in Materials and Manufacturing Engineering, 2006, 17(1−2): 165−168.

[3] TERRONES M. Carbon nanotubes: Synthesis and properties, electronic devices and other emerging applications [J]. International Materials Reviews, 2004, 49: 325−377.

[4] BROZA G. Synthesis, properties, functions and applications of carbon nanotubes: A state of the art review [J]. Chemistry and Chemicals Technology, 2010, 4(1): 35−45.

[5] BAKSHI S R, LAHIRI D. Carbon nanotube reinforced metal matrix composites—A review [J]. International Materials Review, 2010, 55: 41−64.

[6] CHA S I, KIM K T, ARSHAD S N, MO C B, HONG S H. Extraordinary strengthening effect of carbon nanotubes in metal matrix nanocomposites processed by molecular level mixing method [J]. Advance Materials, 2005, 17: 1377−1381.

[7] HU Chang-yuan, XU Ya-juan, DUO Shu-wang, ZHANG Rong-fa, LI Ming-sheng. Non covalent functionalization of carbon nanotubes with surfactants and polymers [J]. Journal of Chinese Chemical Society, 2009, 56: 234−239.

[8] PAL H, SHARMA V, KUMAR R, THAKUR N. Facile synthesis and electrical conductivity of carbon nanotube reinforced nanosilver composites [J]. Z Naturforsch, 2012, 67a: 679−684.

[9] REDDY K R, SIN B C, RYU K S, KIM J C, CHUNG H, LEE Y. Conducting polymer functionalized multiwall carbon nanotubes with novel metal nanoparticles: Synthesis, morphological characteristics and electrical properties[J]. Synthetic Metals, 2009, 159: 595−599.

[10] GOYANES S, RUBIOLO G R, SALAZAR A, JIMENO A, CORCUERA M A, MONDRAGON I. Carboxylation treatment of multiwalled carbon nanotubes monitored by infrared and ultraviolet spectroscopies and scanning probe microscopy [J]. Diamond & Related Materials, 2007, 16: 412−417.

[11] NAKAMIZO M, HONDA H, INAGAKI M. Raman spectra of ground natural graphite [J]. Carbon, 1978, 16: 281−283.

[12] DAVIS W M, ERICKSON C L, JOHNSTON C T, DELFINO J J, PORTER J E. Quantitative Fourier transform infrared spectroscopic investigation of humic substance functional group composition [J]. Chemosphere 1999, 38: 2913−2928.

[13] CHU K, WU Q, JIA C, LIANG X, NIE J, TIAN W, GAI G, GUO H. Fabrication and effective thermal conductivity of multi-walled carbon nanotubes reinforced Cu matrix composites for heat sink applications [J]. Composites Science and Technology, 2010, 70: 298−304.

[14] CHU K, GUO H, JIA C, YIN F, ZHANG X, LIANG X, CHEN H. Thermal properties of carbon nanotube–copper composites for thermal management applications [J]. Nanoscale Research Letters, 2010, 5: 868−874.

[15] KIM K T, ECKERT J, LIU G, PARK J M, LIM B K, HONG S H. Influence of embedded-carbon nanotubes on the thermal properties of copper matrix nanocomposites processed by molecular-level mixing [J]. Scripta Materialia, 2011, 64: 181−184.

[16] CHAI G, CHEN Q. Characterization study of the thermal conductivity of carbon nanotube copper nanocomposites [J]. Journal of Composite Materials, 2010, 44: 2863−2873.

[17] CHU K, JIA C, LI WEN. Thermal conductivity enhancement in carbon nanotube/Cu−Ti composites [J]. Applied physics A, 2013, 110: 269−273.

[18] CHU K, JIA C, JIANG LI, LI WEN. Improvement of interface and mechanical properties in carbon nanotube reinforced Cu–Cr matrix composites [J]. Materials and Design, 2013, 45: 407−411.

[19] BALASUBRAMANIAN K, BURGHARD M. Chemically functionalized carbon nanotubes [J]. Small, 2005, 1(2): 180−192.

[20] KIM K T, CHA S I, GEMMING T, ECKERT J, HONG S H. The role of interfacial oxygen atoms in the enhanced mechanical properties of carbon-nanotube-reinforced metal matrix nanocomposites [J]. Small, 2008, 4(11): 1936−1940.

[21] VAISMAN L, WAGNER H D, MAROM G. The role of surfactants in dispersion of carbon nanotubes [J]. Advances in Colloid and Interface Science, 2006, 128: 37−46.

[22] NAN C W, SHI Z, LIN Y. A simple model for thermal conductivity of carbon nanotube-based composites [J]. Chemical Physics Letters, 2003, 375: 666−669.

[23] NAN C W, LIU G, LIN Y H, LI M. Interface effect on thermal conductivity of carbon nanotube composites [J]. Applied Physics Letters, 2004, 85: 3549−3551.
[24] HUXTABLE S, CAHILL D G, SHENOGIN S, XUE L, OZISIK R, BARONE P. Interfacial heat flow in carbon nanotube suspensions [J]. Nature Mater, 2003, 2: 731−734.
[25] NAN C W, BIRRINGER R, CLARKE D R, GLEITER H. Effective thermal conductivity of particulate composites with interfacial thermal resistance [J]. J Appl Phys, 1997, 81: 6692−6698.

碳纳米管增强银复合材料的导热性

Hemant PAL[1,2], Vimal SHARMA[1]

1. Department of Physics, National Institute of Technology, Hamirpur (H.P.) 177005, India;
2. Department of Physics, Govt. Post Graduate College Chamba (H.P.), 176310, India

摘　要：通过分子水平层级混合制备了碳纳米管增强银基复合材料。研究了碳纳米管的类型(单壁/多壁)及功能化模式(共价键/非共价键)对银复合材料导热性的影响。XRD 及 EDS 结果表明，复合材料中存在银与碳。高分辨率扫描电镜和透射电镜结果表明碳纳米管均匀地嵌在银基体中。利用拉曼光谱和 FTIR 研究了共价键功能化对多壁碳纳米管的影响。共价键功能化后，碳纳米管中引入了功能团且保持结构完整。利用激光闪光技术以及有效介质理论研究了复合材料的导热性。实验结果表明：加入共价功能化的单壁和多壁纳米碳管后，材料的导热性降低。但加入非共价键功能化的多壁碳纳米管后，复合材料的有效导热性增强，这与不考虑界面热阻时的有效介质理论预测结果一致。

关键词：金属基复合材料；碳纳米管；导热性；功能化

(Edited by Yun-bin HE)